



OPEN ACCESS

EDITED BY

Han de Winde,
Leiden University, Netherlands

REVIEWED BY

Zuyi Huang,
Villanova University, United States
Armstrong Ighodalo Omoregie,
University of Technology Malaysia, Malaysia

*CORRESPONDENCE

J. Jordan Steel,
✉ james.steel@afacademy.af.edu

RECEIVED 26 January 2024

ACCEPTED 13 May 2024

PUBLISHED 30 May 2024

CITATION

Vigil TN, Schwendeman NK, Grogger MLM,
Morrison VL, Warner MC, Bone NB, Vance MT,
Morris DC, McElmurry K, Berger BW and Steel JJ
(2024), Surface-displayed silicatein- α enzyme
in bioengineered *E. coli* enables
biocementation and silica mineralization.
Front. Syst. Biol. 4:1377188.
doi: 10.3389/fsysb.2024.1377188

COPYRIGHT

© 2024 Vigil, Schwendeman, Grogger,
Morrison, Warner, Bone, Vance, Morris,
McElmurry, Berger and Steel. This is an open-
access article distributed under the terms of the
[Creative Commons Attribution License \(CC BY\)](https://creativecommons.org/licenses/by/4.0/).
The use, distribution or reproduction in other
forums is permitted, provided the original
author(s) and the copyright owner(s) are
credited and that the original publication in this
journal is cited, in accordance with accepted
academic practice. No use, distribution or
reproduction is permitted which does not
comply with these terms.

Surface-displayed silicatein- α enzyme in bioengineered *E. coli* enables biocementation and silica mineralization

Toriana N. Vigil¹, Nikolas K. Schwendeman²,
Melanie L. M. Grogger^{2,3}, Victoria L. Morrison²,
Margaret C. Warner², Nathaniel B. Bone², Morgan T. Vance²,
David C. Morris², Kristi McElmurry², Bryan W. Berger¹ and
J. Jordan Steel^{2*}

¹Department of Chemical Engineering, University of Virginia, Charlottesville, VA, United States,

²Department of Biology, United States Air Force Academy, Colorado Springs, CO, United States, ³Life Sciences Research Center, United States Air Force Academy, Colorado Springs, CO, United States

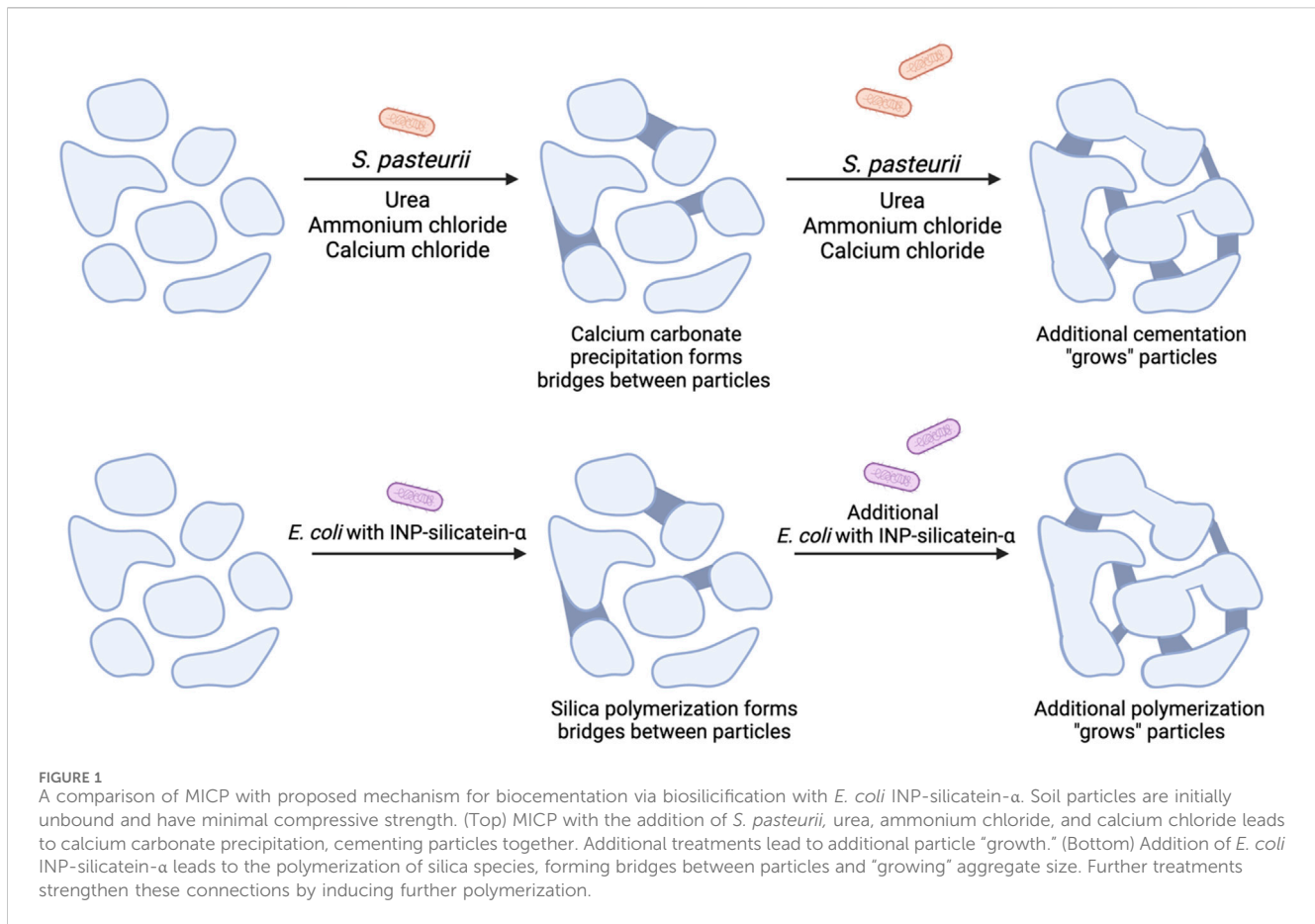
Biocementation is an exciting biomanufacturing alternative to common cement, which is a significant contributor of CO₂ greenhouse gas production. In nature biocementation processes are usually modulated via ureolytic microbes, such as *Sporosarcina pasteurii*, precipitating calcium carbonate to cement particles together, but these ureolytic reactions also produce ammonium and carbonate byproducts, which may have detrimental effects on the environment. As an alternative approach, this work examines biosilicification via surface-displayed silicatein- α in bio-engineered *E. coli* as an *in vivo* biocementation strategy. The surface-display of silicatein- α with ice nucleation protein is a novel protein fusion combination that effectively enables biosilicification, which is the polymerization of silica species in solution, from the surface of *E. coli* bacterial cells. Biosilicification with silicatein- α produces biocementation products with comparable compressive strength as *S. pasteurii*. This biosilicification approach takes advantage of the high silica content found naturally in sand and does not produce the ammonium and carbonate byproducts of ureolytic bacteria, making this a more environmentally friendly biocementation strategy.

KEYWORDS

biocementation, biosilicification, biomineralization, silicatein- α , biotechnology

Introduction

Cement is a key building block for most structures—ranging from basic homes, to skyscraper office buildings, to timeless monuments. Unfortunately, cement is also a major contributor of man-made CO₂ production and a tremendous use of natural resources, resulting in an environmental burden (Gartner and Macphée, 2011; Iqbal et al., 2021). One alternative to man-made cement is microbially induced calcite precipitation (MICP), more commonly known as biocementation. Biocementation usually takes advantage of natural ureolytic and nitrification processes in microbes to precipitate large particle aggregates and can be considered biomanufacturing of cement (Zuo et al., 2023). In the most common usage of MICP, calcium carbonate is precipitated, forming bridges between smaller particles



and "cementing" them together. Biocementation has many applications, including use as a building block for structures, soil stabilization and erosion prevention, and dust mitigation; these functions also make it a prime candidate for future space applications on the moon or Mars (Castro-Alonso et al., 2019; Erdmann and Strieth, 2023; Zuo et al., 2023).

The bacteria *Sporosarcina pasteurii* is frequently used in MICP for its high intrinsic urease activity: breaking down urea and producing ammonia and carbonate (Murugan et al., 2021; Erdmann and Strieth, 2023). Carbonate ions then react with exogenous calcium to form precipitated calcium carbonate, which attaches to nearby particles and can link particles together, effectively increasing aggregate size. While there are a significant number of studies using *S. pasteurii* and MICP, there are two important drawbacks to consider: 1) there is relatively low abundance of calcium in soil and 2) the ammonium and carbonate by-products may have potential adverse environmental impacts (Lee et al., 2019; Gowthaman et al., 2022). MICP with *S. pasteurii* is most effective with 22% w/v calcium content; however, the average calcium content in soil is less than 1.5%, thus necessitating the addition of additional calcium as a reagent for biocementation (Shacklette and Boerngen, 1984; Erdmann and Strieth, 2023). Furthermore, while the production of ammonium and carbonate are crucial for MICP with *S. pasteurii*, these chemicals remain in the environment as pollutants (Yu et al., 2021). An overabundance of ammonium and carbonate in the environment can lead to harmful outcomes, such as algal blooms or local

acidification (J. Gao et al., 2020; Karadag et al., 2006; Su et al., 2022). While biomufacturing cement with MICP may be more eco-friendly than traditional cement production, *S. pasteurii* and ureolytic MICP also have negative side effects such as the buildup of ammonium and carbonate. Here we propose biocementation via biosilicification with surface-displayed silicatein- α in bio-engineered *Escherichia coli* as a more sustainable alternative.

Biocementation via biosilicification may eliminate the requirement for added reagents such as calcium, as silica is present at approximately 30% w/v in standard soil and sand (Shacklette and Boerngen, 1984; Churchman and Lowe, 2012; Cherian and Arnepalli, 2015). Silicatein- α is a biomineralization enzyme that naturally performs silica polymerization in marine sponges (Shimizu et al., 1998). A proposed comparison between traditional MICP and the biosilicification biocementation strategy is shown in Figure 1. Recent work by Gao, et al. highlights silicatein- α precipitation of calcium species in enriched CO₂ and calcium reagent conditions (K. Gao et al., 2024). Work by Wang et al. showed that surface-displayed silicatein in yeast resulted in the formation of a cross-linked matrix of biosilica with embedded yeast cells, supporting our supposition that silicification and not calcium carbonate production is occurring (Wang et al., 2020). The combination of silica and calcium precipitation may lead to enhanced strength in biocementation products and silicatein- α may have a dual use for catalyzing both reactions (K. Gao et al., 2024; Kellermeier et al., 2012). Furthermore, implementing this biosilicification strategy in engineered *E. coli* rather than *S.*

pasteurii allows for future genetic engineering for silica pathway optimization. In this work we show surface-display of silicatein- α in *E. coli* enables biocementation via biosilicification in an easily genetically-modifiable system with limited protein processing and purification steps.

Materials and methods

Plasmid preparation

INP-silicatein- α (INP accession #Q33479.1, silicatein- α accession #CDO33960.1) was cloned into pET-28a (+) plasmid at with standard molecular biology techniques with BamHI and XhoI. INP-silicatein- α pET-28a (+) was transformed into BL21 (DE3) *E. coli* through electroporation of electrocompetent cells. We used a T7 RNA polymerase and isopropyl β -D-1-thiogalactopyranoside (IPTG) induction system for the expression of the INP-silicatein- α protein. To induce INP-silicatein- α expression, starter cultures grown overnight were spun in a centrifuge at 3,000 rcf for 10 min. The supernatant was removed, and the pellet was resuspended in terrific broth with kanamycin and 10 glass disruption beads for aeration. The bacterial culture was then shaken at 250 rpm at 37°C until the culture reached an OD600 of 0.60. At the desired OD600 0.1 mM IPTG was introduced to the culture for induction of the INP-silicatein- α protein. The culture was then left shaking at room temperature overnight.

SDS-PAGE

E. coli INP-silicatein- α cell culture was pelleted via centrifugation, then resuspended in sonication lysis buffer (5 mL/1 g cell pellet) consisting of glycerol (99%) (5% v/v), tris HCl (36 mM), tris base (20 mM), NaCl (100 mM), and imidazole (5 mM). The sample was sonicated via micro-tip sonification at 20% amplitude for 20 min in on/off intervals of 20 s on ice. Following lysis, the lysate was clarified via centrifugation at 10,000 rcf for 10 min. A sample of clarified lysate was then denatured using a thermocycler at 95°C. A 10% Mini-PROTEAN TGX Precast Protein Gel was loaded with serial dilutions of lysed *E. coli* INP-silicatein- α and Laemmli buffer containing β -mercaptoethanol totaling to 20 μ L in each well. One well was loaded with a Bio-Rad Precision Plus Protein ladder. After running the gel at 150 V for 50 min, the gel was fixed with a 50% H₂O, 40% methanol, and 10% acetic acid solution. The gel was then stained with Bio-Safe™ Coomassie Stain, destained with DI H₂O, and an image was captured using a Bio-Rad Gel Doc XR+ Gel Documentation System.

Western blot

Following the SDS-PAGE procedure, the proteins were then transferred to nitrocellulose through a Bio-Rad Criterion Blotter apparatus. The nitrocellulose was incubated in 1x EveryBlot Blocking Buffer (BioRad) for at least 5 min. Then anti-penta-his conjugated HRP antibody (BioRad) diluted 1/1000 was added and

incubated for 1 h. The membrane was rinsed gently with 0.1% Tween 20 tris-buffered saline for 3 min and treated with ECL solution (Amersham). Membrane was then imaged with chemiluminescence.

Immunocytochemistry

After protein expression, the culture was spun down at 3,000 rcf for 10 min. The pellet was then washed twice with tris-buffered saline and resuspended in 100% ice cold methanol, a nonpermeabilizing fixative. After incubating in methanol on ice for 10 min, 100 μ L were dropped on a slide and dried. Anti-silicatein- α rabbit unconjugated primary antibody (antibodies.com A81861) diluted in 1/1,000 EveryBlot blocking buffer (BioRad) was added. Slides were then transferred to a humidifying chamber at 4°C overnight. The next day, the slides were washed with tris-buffered saline and anti-rabbit goat AlexaFluor 488 secondary antibody (Invitrogen A27034) diluted 1/10,000 in EveryBlot blocking buffer (BioRad) was added. Slides were incubated for at 37°C 1 h, washed again with tris-buffered saline, and a coverslip was added with ProLong Gold Antifade Mountant with DNA Stain DAPI (ThermoFisher Scientific P3693). The slides were imaged on a Keyence BZ-X810 Fluorescence Microscope with a $\times 60$ objective lens.

In vivo biomineralization

5 mL of induced INP-silicatein- α in *E. coli* cultures was spun down at 3,000 rcf for 10 min. The cell pellet was resuspended in 25 mL of sterile, DI H₂O in a 125 mL flask. A final concentration of 2 mM sodium orthosilicate was added. Mixture was incubated overnight at room temperature shaking. A WT BL21 *E. coli* and sodium orthosilicate only control were included. After 24 h, cells were removed from solution via centrifugation at 1,000 \times g for 10 min. The supernatant was ultracentrifuged in 5 mL increments at 50,000 \times g for 45 min to precipitate silica biomineralization products.

Silicomolybdate assay

Following ultracentrifugation, samples were dried and resuspended in 0.2 M NaOH. Samples were then adjusted to pH 1.6–1.9 with 2 M HCl. After recording total sample volume, samples were transferred to 96-well plate in 200 μ L increments. 15 μ L of 5% w/v ammonium molybdate was added to each well then incubated at RT for 15 min 15 μ L of 0.1% w/v ascorbic acid and 15 μ L of 0.1% w/v oxalic acid were added to each well and incubated at RT for 2 h. Absorbance was read at 820 nm on BioTek Synergy Neo2 plate reader. Nanograms of silica were calculated via Beer's Law with extinction coefficient 44,710 mol⁻¹ cm⁻¹ as derived previously (Coradin, T., Eglin, D., Livage, 2004).

S. pasteurii growth

Sporosarcina pasteurii (ATCC 11859/DSM 33) cultures were revived from glycerol stocks (5–10 μ L) and resuspended with 5 mL

of Bacto™ Brain Heart Infusion supplemented with urea (0.3 M). The cultures were grown at room temperature (25°C) overnight (12–16 hrs), shaking.

Brick construction

In order to construct biocemented bricks, Sandstastik Sparkling White Play Sand (Flinn Scientific #AP9567) was poured into a 3-inch (height) by 1.5-inch (diameter) cylindrical mold lined with stainless steel mesh. 40 mL of cell culture (*S. pasteurii* or *E. coli* INP-silicatein- α) was added dropwise via serological pipette on top of the sand. After waiting 45 min for the culture to fully percolate through the mold, 80 mL of cementation solution was added dropwise via serological pipette. Cementation solution contains urea (0.3 M), ammonium chloride (0.2 M), and calcium chloride dihydrate (0.9 M). 30 min after adding the cementation solution, the next round of biocementation was initiated by dripping 40 mL of cell culture on top of the sand. Three total rounds were completed for each brick. Bricks were left to dry in their mold for 24 h and then removed from the mold and left to cure for 21 days prior to running the unconfined compression test. (Note: although cementation solution is not necessary for silicification with *E. coli* INP-silicatein- α , cementation was applied to these bricks to ensure consistency across experiments and effectively compare the role of *S. pasteurii* and *E. coli* INP-silicatein- α .)

3D printing for brick molds

We designed and created the 3-inch (height) by 1.5-inch (diameter) cylindrical molds using a Stratasys Object30 V5 Pro 3D Printer. SolidWorks software was used to design the molds and create a CAD file. Stratasys' Rigur™ (RGD450) material was used for the molds. After printing, molds were water blasted to remove any structural print residue. Molds were dried for at least 24 h before use for biocementation. Our 3D printed mold design is available upon request to corresponding author.

Unconfined compression tests

To test the compressive strength of the biocemented bricks, each brick was crushed with an ELE International Versa-Loader (model: 25-3525/02) and a model 20210-500 Type S load cell. [Unconfined Compression Test Digital Readout Set, English 110 vAC (271121/02)]. Each brick was placed alone on the lower loading plate, oriented for axial loading with the circular faces flush against the loading plates. Once bricks were placed on the lower loading plate, about 1 pound of pressure was applied to the brick to secure it in place against both upper and lower loading plates. The digital readout was then tared and the test was commenced. Increasing load was continuously applied [approximately 0.08" (2.032 mm) per minute] until complete structural failure of the brick was achieved, which is detected by the instrument as a sudden decrease in compressive load. The highest compressive load observed in the trial was recorded.

Results

For effective *in vivo* biosilicification, we designed a surface-display system with silicatein- α expression in *E. coli*. Previous work by Curnow, et al. (2005) utilized a silicatein- α fusion with the outer membrane protein OmpA for the synthesis of titanium phosphates (Curnow et al., 2005; 2006), but did not attempt biocementation. To our knowledge, there have been no other reports of surface-display with silicatein- α for *in vivo* biomineralization. A comparative study of cell-surface display systems by Nicchi, et. al highlights that the success of various cell-surface display systems cannot be predicted *a priori*, and surface display is best tested *in vivo* (Nicchi et al., 2021). Ice nucleation protein (INP) is a surface protein native to *Pseudomonas syringae* with N and C terminals separated by a varying number of spacer domains (Van Bloois et al., 2011). Previous studies have shown that the N domain alone can facilitate surface-display in *E. coli* with protein cargoes of varying sizes (Van Bloois et al., 2011). Therefore, we fused the N domain of INP with a truncated silicatein- α from *Tethya aurantia*. Recent work by Godigamuwa, et al. fuses silicatein- α with surface display protein *InaK* (often considered identical or analogous to INP), but rather than utilizing silicatein- α as a surface-displayed protein for *in vivo* activity, purifies the protein via established techniques (Godigamuwa et al., 2023). With the exception of the SDS-PAGE gel and Western blot to highlight protein expression, INP-silicatein- α was used *in vivo* for this work.

INP-silicatein- α expression was confirmed with SDS-PAGE and Western blot (Figure 2), with bands at approximately 51.5 kDa and 103 kDa. The band at 103 kDa is consistent with protein dimerization, which is unsurprising given that the native purpose of INP (ice nucleation) relies on oligomerization of protein structure (Garnham et al., 2011; Hartmann et al., 2022). Importantly, protein purification will not be necessary for application of INP-silicatein- α in biocementation, as the surface-display enables access to the enzyme while also providing some measure of stability. Surface protein expression and accessibility without purification is advantageous by limiting post-processing steps required for application.

To visualize INP-silicatein- α expression on the surface of the cells, we examined the cells with fluorescence microscopy following immunocytochemistry. An anti-silicatein- α antibody with AlexaFluor 488 was used to target silicatein- α expression on the surface of the cell. Membrane-permeable DAPI staining for nucleic acids was subsequently performed to highlight the interior of the cell. Figure 3 compares WT BL21 *E. coli* and *E. coli* INP-silicatein- α , illustrating DAPI staining in both samples, but green fluorescence only in cells expressing the INP-silicatein- α . These results verify that INP-silicatein- α is surface displayed and therefore accessible to substrates for biomineralization activity.

In vivo biomineralization was evaluated by introducing the common silica precursor sodium orthosilicate directly to *E. coli* INP-silicatein- α . Previous work shows direct biomineralization of inorganic silica precursors following incubation with silicatein- α over a period of 24 h at room temperature (Cha et al., 1999; Muller et al., 2008; Curran et al., 2017; Povarova et al., 2018). Following 24-h room-temperature incubation with silica precursor and subsequent ultra-centrifugation, mineralized silica was collected from *E. coli* INP-silicatein- α (Figure 4). Sodium orthosilicate

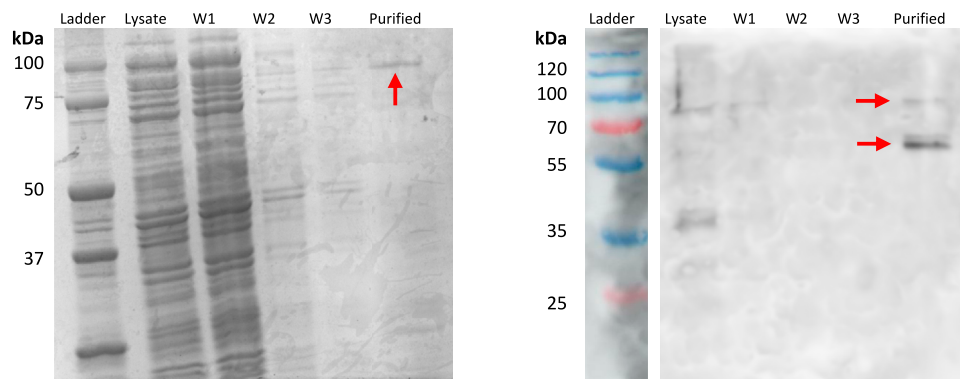


FIGURE 2
SDS-PAGE and Western blot highlighting INP-silicatein- α expression. SDS-PAGE for INP-silicatein- α purification with cell lysate, wash 1 (W1), wash 2 (W2), wash 3 (W3), and purified fractions. Western blot shows lysate, W1, W2, W3, and purified fractions. Red arrows indicate bands consistent with anticipated molecular weight of INP-silicatein- α (51.5 kDa) and INP-silicatein- α dimer (103 kDa).

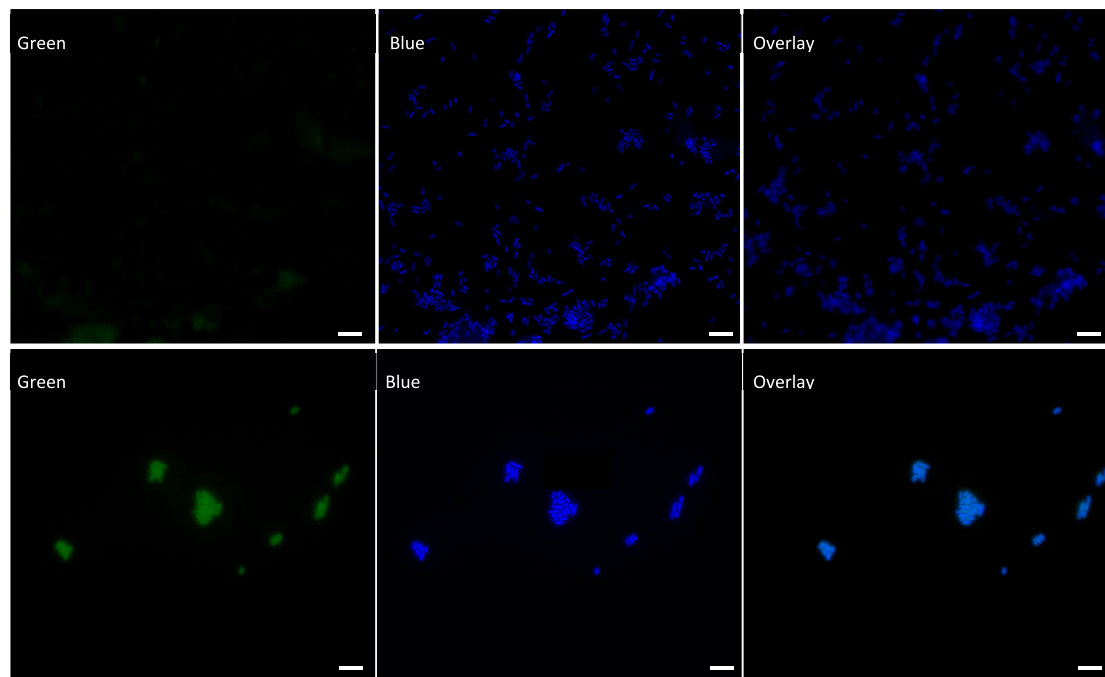


FIGURE 3
Immunocytochemistry of WT BL21 *E. coli* and *E. coli* INP-silicatein- α . Green fluorescence shows AlexaFluor 488 conjugated to anti-silicatein- α . Blue fluorescence shows DAPI staining of nucleic acids, highlighting the interior of bacterial cells. Overlay shows co-localization of INP-silicatein- α on the exterior of DAPI-stained cells for *E. coli* INP-silicatein- α , but not on WT BL21 *E. coli*.

precursor treated under the same conditions (without *E. coli* INP-silicatein- α) did not yield any precipitate. A quantitative measure of precipitate via silicomolybdate assay reveals that silica precipitation with *E. coli* INP-silicatein- α is significantly greater than with WT BL21 *E. coli* (unpaired t-test: $t = 16.93$, $d.f. = 2$, $p = 0.0035$), indicating that surface-displayed silicatein- α is biomineralization active. These results are promising for *in vivo* applications with surface-displayed silicatein- α , and effectively eliminates the need for protein purification, making biomineralization with silicatein- α less time and resource intensive.

Biocementation products such as bricks and columns are often used to measure strength and physical properties from the biocementation (Bachmeier et al., 2002; Zhao et al., 2014; Cardoso et al., 2020; Erdmann et al., 2022; Spencer et al., 2023). Compressive strength testing of cylindrical bricks made with *S. pasteurii* or *E. coli* INP-silicatein- α revealed encouraging results for the development of a silica-based biocementation pathway. As part of this work, WT BL21 *E. coli* treated bricks (without INP-silicatein- α expression) did not retain enough structure for unconfined compression testing, thus illustrating that *E. coli* alone does not

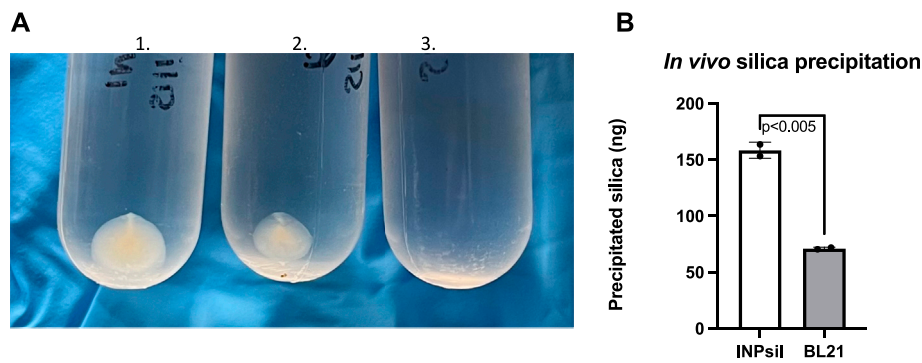


FIGURE 4

In vivo biomineralization with INP-silicatein- α . Silica mineralization can be visualized as precipitate after sample ultra-centrifugation. (A) 1) Precipitate from *E. coli* INP-silicatein- α and sodium orthosilicate after 24-h incubation, 2) precipitate from WT BL21 *E. coli* and sodium orthosilicate after 24-h incubation, 3) precipitate from sodium orthosilicate alone after 24-h incubation. (B) Comparison of precipitated silica (ng) as quantified via silicomolybdate assay. Two-tailed unpaired t-test ($p < 0.005$).

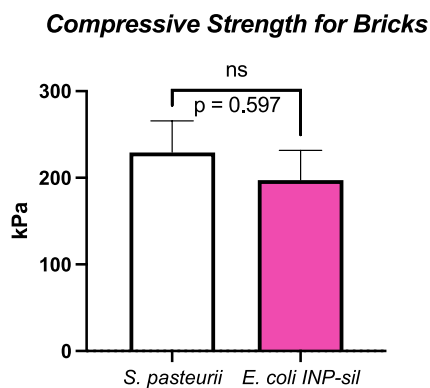


FIGURE 5

Unconfined compressive strengths for *S. pasteurii* and *E. coli* INP-silicatein- α bricks. *S. pasteurii* bricks show an average tolerance to 229 kPa (S.E.M. 36 kPa). *E. coli* INP-silicatein- α bricks show an average tolerance of 197 kPa (S.E.M. 34 kPa). A two-tailed unpaired t-test shows no significant difference between the two ($p = 0.597$).

have biocementation properties. (Non-cohesive soils like sand cannot be accurately measured in an unconfined compression test because they will immediately fall apart.) Similar results have been reported previously, highlighting the lack of urease activity and subsequent calcium carbonate precipitation associated with *E. coli* (Bachmeier et al., 2002; Liang et al., 2018; Heveran et al., 2019).

S. pasteurii and *E. coli* INP-silicatein- α bricks withstood an average of 229 kPa (S.E.M. 36 kPa) and 197 kPa (S.E.M. 34 kPa), respectively (Figure 5). These compressive strengths are comparable to Type A soils, the most stable soil category as defined by OSHA (OSHA Technical Manual (OTM), 2014). Sand alone (i.e., bricks prior to treatment with *S. pasteurii* or *E. coli* INP-silicatein- α), is considered a Type C soil, thus illustrating that the two different modes of bacterial biocementation explored here had significant impacts on soil cohesion. Furthermore, two-tailed unpaired t-test analysis, showed that the compressive strength of the two brick types did not differ significantly from each other (unpaired t-test: $t = 0.5407$, d.f. = 14, $p = 0.59$). The lack of a significant difference informs us that the two pathways yield

comparable results and that a silica-centric biocementation pathway may be a viable option.

Discussion

Notably, the cementation solution treatments containing urea and ammonium chloride may hinder *E. coli* viability and subsequent activity of INP-silicatein- α , thereby impeding silica formation. Higher concentrations of urea, such as in our cementation solution, have been shown to be toxic and inhibit growth of *E. coli* (Weinstein and McDonald, 1945; Schlegel et al., 1961; Taabodi et al., 2019). Alternatively, it is possible that the high levels of urea and ammonium chloride introduce porosity into the biomineralized silica structure (Kot et al., 2021), thereby weakening the biocementation product. In spite of this, cementation solution was applied to *E. coli* INP-silicatein- α as with *S. pasteurii*, to ensure that comparisons between the unconfined compressive strength could be credited to the different *E. coli* INP-silicatein- α and *S. pasteurii* microbes. Figure 5 shows that the unconfined compressive strength between bricks made with *S. pasteurii* and bricks made with *E. coli* INP-silicatein- α are not significantly different, highlighting the promising potential for INP-silicatein- α biosilicification in biocementation. We are currently testing to find the optimal conditions for biocementation with silica, including removing the urea and calcium cementation solutions in order to mitigate the production of harmful byproducts from traditional MICP.

The use of biocementation for cement production, improving soil strength, and dust mitigation is becoming increasingly possible with new and emerging research, with many studies applying biocementation techniques to stabilizing loose sediment via “grouting,” sealing undeveloped roads, encapsulating pollutants, preserving historical stone structures, and even CO₂ fixation (Dharmi et al., 2014; Anbu et al., 2016; Portugal et al., 2020). Biocementation may also be necessary in efforts to colonize other planets. One major roadblock for building structures on the moon or Mars is the cost of shipping tons of cement into space. *In situ* resource utilization strives to use the resources already present with minimal added materials. Implementing INP-silicatein- α expression in cyanobacteria, which research suggests can grow using only resources found on Mars and

may thrive in space (Verseux et al., 2021; Mapstone et al., 2022; Ramalho et al., 2022), may be an avenue for biocementation, providing a necessary foundation for extraterrestrial construction at a relatively small cost. Lunar and martian regolith have calcium and silica content of approximately 14% and 49%, respectively (Exolith Lab, 2023), which suggests that biocementation via biosilicification may be a suitable target.

Additionally, the expression of a silica biocementation pathway in *E. coli* rather than *S. pasteurii* allows for future genetic engineering optimization and greater enhancement of the silica pathway. *E. coli* has proven to be an ideal platform host for development of industrially viable productions (Pontrelli et al., 2018). While *S. pasteurii* relies on a narrow pH range, more specific temperature, and precise urea concentrations for optimal biocementation, *E. coli* can be more easily genetically modified to adjust to different environmental conditions (Dong et al., 2023). Improvements and optimization of the silica biocementation pathway through *E. coli* can bring us one step closer to biomanufactured cement for space applications. Figure 5 shows that biosilicification with INP-silicatein- α is a promising alternative to biocementation with *S. pasteurii* as there is no significant difference between unconfined compression strength of bricks made with each. Upon optimization of INP-silicatein- α in *E. coli*, this system can be adapted for expression in cyanobacteria. Cyanobacteria may potentially provide numerous benefits in improvement of this system; they are photosynthetic, potentially providing an additional source of oxygen in extraterrestrial environment, and different strains have evolved to withstand more extreme conditions and stressors—high and low temperatures, desiccation, variable pH, and fluctuating salinity (Berla et al., 2013). The ability for cyanobacteria to survive and grow in hostile environments, combined with biosilicification activity, could make biocementation on distant planets a reality.

In the future, optimization experiments for biosilicification with *E. coli* INP-silicatein- α can assess silica mineralization with varying conditions and timescales. Further details such as any potential effects from local bacterial populations or potential effects from *E. coli* INP-silicatein- α survival in lab or field environments should be examined to further enhance the efficiency and long-term impacts of biocementation via biosilicification. These studies will lay the foundation for future biocementation applications and research.

Data availability statement

The original contributions presented in the study are included in the article/Supplementary material, further inquiries can be directed to the corresponding author.

Author contributions

TV: Conceptualization, Data curation, Formal Analysis, Funding acquisition, Investigation, Methodology, Supervision, Validation, Visualization, Writing—original draft, Writing—review and editing. NS: Data curation, Investigation, Methodology, Resources, Validation, Visualization, Writing—original draft, Writing—review and editing. MG: Conceptualization, Data curation, Formal Analysis, Investigation, Methodology, Project administration, Resources,

Supervision, Validation, Visualization, Writing—review and editing. VM: Conceptualization, Data curation, Formal Analysis, Funding acquisition, Investigation, Methodology, Project administration, Resources, Supervision, Validation, Visualization, Writing—review and editing. MW: Conceptualization, Data curation, Investigation, Methodology, Validation, Visualization, Writing—review and editing. NB: Investigation, Methodology, Resources, Writing—review and editing. MV: Methodology, Resources, Software, Writing—review and editing. DM: Conceptualization, Project administration, Supervision, Writing—review and editing. KM: Conceptualization, Investigation, Project administration, Writing—review and editing. BB: Formal Analysis, Funding acquisition, Project administration, Resources, Writing—review and editing. JS: Conceptualization, Funding acquisition, Investigation, Methodology, Project administration, Resources, Supervision, Writing—review and editing.

Funding

The author(s) declare that financial support was received for the research, authorship, and/or publication of this article. This material is based on work supported by the National Science Foundation under Grant No. 1727166 (TV), 1821389 (TV), and research agreement No. FA7000-19-2-0035 (MG). Additionally, the Department of Defense (DoD) STEM National Defense Education Program (NDEP) grant titled Biotechnology Outreach Bolstered through Education in STEM and Development (BiOBESTD) HQ0642265477 helped fund iGEM and research supplies.

Acknowledgments

We would like to thank Col Steven Hasstedt, Basic Science Division chair, and Gen Linell Letendre, Dean of the US Air Force Academy, for their continual support for the USAFA iGEM team. Dr. Armand Balboni, Life Science Research Center Director, for his support in acquiring and managing funding. We also acknowledge the other iGEM team members from past and present USAFA iGEM teams and our collaborators at the Air Force Research Labs that helped with training, advice, and general guidance with the research project.

Conflict of interest

The authors declare that the research was conducted in the absence of any commercial or financial relationships that could be construed as a potential conflict of interest.

The author(s) declared that they were an editorial board member of Frontiers, at the time of submission. This had no impact on the peer review process and the final decision.

Author disclaimer

The views expressed in this paper are those of the authors and do not necessarily represent the official position or policy of the U.S. Government, the Department of Defense, or the Department of the Air Force.

Publisher's note

All claims expressed in this article are solely those of the authors and do not necessarily represent those of their affiliated

organizations, or those of the publisher, the editors and the reviewers. Any product that may be evaluated in this article, or claim that may be made by its manufacturer, is not guaranteed or endorsed by the publisher.

References

- Anbu, P., Kang, C.-H., Shin, Y.-J., and So, J.-S. (2016). Formations of calcium carbonate minerals by bacteria and its multiple applications. *SpringerPlus* 5 (1), 250. doi:10.1186/s40064-016-1869-2
- Bachmeier, K. L., Williams, A. E., Warmington, J. R., and Bang, S. S. (2002). Urease activity in microbiologically-induced calcite precipitation. *J. Biotechnol.* 93 (2), 171–181. doi:10.1016/S0168-1656(01)00393-5
- Berla, B. M., Saha, R., Immethun, C. M., Maranas, C. D., Moon, T. S., and Pakrasi, H. B. (2013). Synthetic biology of cyanobacteria: unique challenges and opportunities. *Front. Microbiol.* 4, 246. doi:10.3389/fmicb.2013.00246
- Cardoso, R., Pedreira, R., Duarte, S. O. D., and Monteiro, G. A. (2020). About calcium carbonate precipitation on sand biocementation. *Eng. Geol.* 271, 105612. doi:10.1016/j.enggeo.2020.105612
- Castro-Alonso, M. J., Montañez-Hernandez, L. E., Sanchez-Muñoz, M. A., Macias Franco, M. R., Narayanasamy, R., and Balagurusamy, N. (2019). Microbially induced calcium carbonate precipitation (MICP) and its potential in biocement: microbiological and molecular concepts. *Front. Mater.* 6, 126. doi:10.3389/fmats.2019.00126
- Cha, J. N., Shimizu, K., Zhou, Y., Christiansen, S. C., Chmelka, B. F., Stucky, G. D., et al. (1999). Silicatein filaments and subunits from a marine sponge direct the polymerization of silica and silicones *in vitro*. *Proc. Natl. Acad. Sci. U. S. A.* 96 (2), 361–365. doi:10.1073/pnas.96.2.361
- Cherian, C., and Arnepalli, D. N. (2015). A critical appraisal of the role of clay mineralogy in lime stabilization. *Int. J. Geosynth. Ground Eng.* 1 (1), 8. doi:10.1007/s40891-015-0009-3
- Churchman, G. J., and Lowe, D. J. (2012). "Alteration, formation, and occurrence of minerals in soils," in *Handbook of Soil Sciences: Properties and Processes*. (CRC Press), 1–72. Available at: <https://hdl.handle.net/10289/9024>.
- Coradin, T., Eglin, D., and Livage, J. (2004). The silicomolybdc acid spectrophotometric method and its application to silicate/biopolymer interaction studies. *Spectroscopy* 18, 567–576. doi:10.1155/2004/356207
- Curnow, P., Bessette, P. H., Kisailus, D., Murr, M. M., Daugherty, P. S., and Morse, D. E. (2005). Enzymatic synthesis of layered titanium phosphates at low temperature and neutral pH by cell-surface display of silicatein- α . *J. Am. Chem. Soc.* 127 (45), 15749–15755. doi:10.1021/ja054307f
- Curnow, P., Kisailus, D., and Morse, D. E. (2006). Biocatalytic synthesis of poly(L-lactide) by native and recombinant forms of the silicatein enzymes. *Angew. Chem. Int. Ed.* 45 (4), 613–616. doi:10.1002/anie.200502738
- Curran, C. D., Lu, L., Jia, Y., Kiely, C. J., Berger, B. W., and McIntosh, S. (2017). Direct single-enzyme biomimetic mineralization of catalytically active ceria and ceria-zirconia nanocrystals. *ACS Nano* 11 (3), 3337–3346. doi:10.1021/acsnano.7b00696
- Dhami, N. K., Reddy, M. S., and Mukherjee, A. (2014). Application of calcifying bacteria for remediation of stones and cultural heritages. *Front. Microbiol.* 5, 304. doi:10.3389/fmicb.2014.00304
- Dong, Y., Gao, Z., Wang, D., Di, J., Guo, X., Yang, Z., et al. (2023). Optimization of growth conditions and biological cementation effect of *Sporosarcina pasteurii*. *Constr. Build. Mater.* 395, 132288. doi:10.1016/j.conbuildmat.2023.132288
- Erdmann, N., De Payrebrune, K. M., Ulber, R., and Strieth, D. (2022). Optimizing compressive strength of sand treated with MICP using response surface methodology. *SN Appl. Sci.* 4 (10), 282. doi:10.1007/s42452-022-05169-8
- Erdmann, N., and Strieth, D. (2023). Influencing factors on ureolytic microbiologically induced calcium carbonate precipitation for biocementation. *World J. Microbiol. Biotechnol.* 39 (2), 61. doi:10.1007/s11274-022-03499-8
- OSHA Technical Manual (OTM) (2014). *Excavations: Hazard Recognition in Trenching and Shoring Section V: Chapter 2*. Occupational Safety and Health Administration. Available at: <https://www.osha.gov/otm/section-5-construction-operations/chapter-2>.
- Exolith Lab (2023). *LHS-1 lunar highlands simulant fact sheet*. (003-01-001-1223) [dataset].
- Gao, J., Liu, L., Ma, N., Yang, J., Dong, Z., Zhang, J., et al. (2020). Effect of ammonia stress on carbon metabolism in tolerant aquatic plant—*Myriophyllum aquaticum*. *Environ. Pollut.* 263, 114412. doi:10.1016/j.envpol.2020.114412
- Gao, K., Suleiman, M. T., Brown, D. G., Sadeghnejad, A., and Lin, H. (2024). *Bio-inspired soil Improvement using silicatein- α enzyme* [preprint]. *Review*. doi:10.21203/rs.3.rs-3832275/v1
- Garnham, C. P., Campbell, R. L., Walker, V. K., and Davies, P. L. (2011). Novel dimeric β -helical model of an ice nucleation protein with bridged active sites. *BMC Struct. Biol.* 11 (1), 36. doi:10.1186/1472-6807-11-36
- Gartner, E. M., and Macphee, D. E. (2011). A physico-chemical basis for novel cementitious binders. *Cem. Concr. Res. 41* (7), 736–749. doi:10.1016/j.cemconres.2011.03.006
- Godigamuwa, K., Nakashima, K., Tsujitani, S., Naota, R., Maulidin, I., and Kawasaki, S. (2023). Interfacial biosilica coating of chitosan gel using fusion silicatein to fabricate robust hybrid material for biomolecular applications. *J. Mater. Chem. B* 11 (8), 1654–1658. doi:10.1039/D2TB02581G
- Gowthaman, S., Mohsenzadeh, A., Nakashima, K., and Kawasaki, S. (2022). Removal of ammonium by-products from the effluent of bio-cementation system through struvite precipitation. *Mater. Today Proc.* 61, 243–249. doi:10.1016/j.matpr.2021.09.013
- Hartmann, S., Ling, M., Dreyer, L. S. A., Zipori, A., Finster, K., Grawe, S., et al. (2022). Structure and protein-protein interactions of ice nucleation proteins drive their activity. *Front. Microbiol.* 13, 872306. doi:10.3389/fmicb.2022.872306
- Heveran, C. M., Liang, L., Nagarajan, A., Hubler, M. H., Gill, R., Cameron, J. C., et al. (2019). Engineered ureolytic microorganisms can tailor the morphology and nanomechanical properties of microbial-precipitated calcium carbonate. *Sci. Rep.* 9 (1), 14721. doi:10.1038/s41598-019-51133-9
- Iqbal, D. M., Wong, L. S., and Kong, S. Y. (2021). Bio-cementation in construction materials: a review. *Materials* 14 (9), 2175. doi:10.3390/ma14092175
- Karadag, D., Koc, Y., Turan, M., and Armagan, B. (2006). Removal of ammonium ion from aqueous solution using natural Turkish clinoptilolite. *J. Hazard. Mater.* 136 (3), 604–609. doi:10.1016/j.jhazmat.2005.12.042
- Kellermeier, M., Cölfen, H., and García-Ruiz, J. M. (2012). Silica biomorphs: complex biomimetic hybrid materials from "sand and chalk". *Eur. J. Inorg. Chem.* 2012 (32), 5123–5144. doi:10.1002/ejic.201201029
- Kot, M., Wojcieszak, R., Janiszewska, E., Pietrowski, M., and Zieliński, M. (2021). Effect of modification of amorphous silica with ammonium agents on the physicochemical properties and hydrogenation activity of Ir/SiO₂ catalysts. *Materials* 14 (4), 968. doi:10.3390/ma14040968
- Lee, M., Gomez, M. G., San Pablo, A. C. M., Kolbus, C. M., Graddy, C. M. R., DeJong, J. T., et al. (2019). Investigating ammonium by-product removal for ureolytic bio-cementation using meter-scale experiments. *Sci. Rep.* 9 (1), 18313. doi:10.1038/s41598-019-54666-1
- Liang, L., Heveran, C., Liu, R., Gill, R. T., Nagarajan, A., Cameron, J., et al. (2018). Rational control of calcium carbonate precipitation by engineered *Escherichia coli*. *ACS Synth. Biol.* 7 (11), 2497–2506. doi:10.1021/acssynbio.8b00194
- Mapstone, L. J., Leite, M. N., Purton, S., Crawford, I. A., and Dartnell, L. (2022). Cyanobacteria and microalgae in supporting human habitation on Mars. *Biotechnol. Adv.* 59, 107946. doi:10.1016/j.biotechadv.2022.107946
- Muller, W., Engel, S., Wang, X., Wolf, S., Tremel, W., Thakur, N., et al. (2008). Biocapsulation of living bacteria (*Escherichia coli*) with poly(silicate) after transformation with silicatein- α gene. *Biomaterials* 29 (7), 771–779. doi:10.1016/j.biomaterials.2007.10.038
- Murugan, R., Suraishkumar, G. K., Mukherjee, A., and Dhami, N. K. (2021). Influence of native ureolytic microbial community on biocementation potential of *Sporosarcina pasteurii*. *Sci. Rep.* 11 (1), 20856. doi:10.1038/s41598-021-00315-5
- Nicchi, S., Giuliani, M., Giusti, F., Pancotto, L., Maione, D., Delany, I., et al. (2021). Decorating the surface of *Escherichia coli* with bacterial lipoproteins: a comparative analysis of different display systems. *Microb. Cell Factories* 20 (1), 33. doi:10.1186/s12934-021-01528-z
- Pontrelli, S., Chiu, T.-Y., Lan, E. I., Chen, F. Y.-H., Chang, P., and Liao, J. C. (2018). *Escherichia coli* as a host for metabolic engineering. *Metab. Eng.* 50, 16–46. doi:10.1016/j.jymben.2018.04.008
- Portugal, C. R. M. E., Fonyo, C., Machado, C. C., Meganck, R., and Jarvis, T. (2020). Microbiologically Induced Calcite Precipitation biocementation, green alternative for roads – is this the breakthrough? A critical review. *J. Clean. Prod.* 262, 121372. doi:10.1016/j.jclepro.2020.121372
- Povarova, N. V., Barinov, N. A., Baranov, M. S., Markina, N. M., Varizhuk, A. M., Pozmogova, G. E., et al. (2018). Efficient silica synthesis from tetra(glycerol)orthosilicate with cathepsin- and silicatein-like proteins. *Sci. Rep.* 8 (1), 16759–9. doi:10.1038/s41598-018-34965-9

- Ramalho, T. P., Chopin, G., Pérez-Carrascal, O. M., Tromas, N., and Verseux, C. (2022). Selection of *Anabaena* sp. PCC 7938 as a cyanobacterium model for biological ISRU on Mars. *Appl. Environ. Microbiol.* 88 (15), e0059422–22. doi:10.1128/aem.00594-22
- Schlegel, J. U., Cuellar, J., and O'Dell, R. M. (1961). Bactericidal effect of urea. *J. Urology* 86 (6), 819–822. doi:10.1016/S0022-5347(17)65264-9
- Shacklette, H. T., and Boerngen, J. G. (1984). *Element concentrations in soil and other surficial materials of the conterminous United States (U.S. Geological survey professional paper 1270). United States department of the interior.*
- Shimizu, K., Cha, J., Stucky, G. D., and Morse, D. E. (1998). Silicatein alpha: cathepsin L-like protein in sponge biosilica. *Proc. Natl. Acad. Sci. U. S. A.* 95 (11), 6234–6238. doi:10.1073/pnas.95.11.6234
- Spencer, C. A., Sass, H., and Van Paassen, L. (2023). Increased microbially induced calcium carbonate precipitation (MICP) efficiency in multiple treatment sand biocementation processes by augmentation of cementation medium with ammonium chloride. *Geotechnics* 3 (4), 1047–1068. doi:10.3390/geotechnics3040057
- Su, F., Yang, Y., Qi, Y., and Zhang, H. (2022). Combining microbially induced calcite precipitation (MICP) with zeolite: a new technique to reduce ammonia emission and enhance soil treatment ability of MICP technology. *J. Environ. Chem. Eng.* 10 (3), 107770. doi:10.1016/j.jece.2022.107770
- Taabodi, M., Hashem, F. M., Oscar, T. P., Parveen, S., and May, E. B. (2019). The possible roles of *Escherichia coli* in the nitrogen cycle. *Int. J. Environ. Res.* 13 (3), 597–602. doi:10.1007/s41742-019-00191-y
- Van Bloois, E., Winter, R. T., Kolmar, H., and Fraaije, M. W. (2011). Decorating microbes: surface display of proteins on *Escherichia coli*. *Trends Biotechnol.* 29 (2), 79–86. doi:10.1016/j.tibtech.2010.11.003
- Verseux, C., Heinicke, C., Ramalho, T. P., Determann, J., Duckhorn, M., Smagin, M., et al. (2021). A low-pressure, N₂/CO₂ atmosphere is suitable for cyanobacterium-based life-support systems on Mars. *Front. Microbiol.* 12, 611798. doi:10.3389/fmicb.2021.611798
- Wang, H., Wang, Z., Liu, G., Cheng, X., Chi, Z., Madzak, C., et al. (2020). Genetical surface display of silicatein on *Yarrowia lipolytica* confers living and renewable biosilica–yeast hybrid materials. *ACS Omega* 5 (13), 7555–7566. doi:10.1021/acsomega.0c00393
- Weinstein, L., and McDonald, A. (1945). The effect of urea, urethane and other carbamates on bacterial growth. *Science* 101 (2611), 44–45. doi:10.1126/science.101.2611.44
- Yu, X., Chu, J., Yang, Y., and Qian, C. (2021). Reduction of ammonia production in the biocementation process for sand using a new biocement. *J. Clean. Prod.* 286, 124928. doi:10.1016/j.jclepro.2020.124928
- Zhao, Q., Li, L., Li, C., Li, M., Amini, F., and Zhang, H. (2014). Factors affecting improvement of engineering properties of MICP-treated soil catalyzed by bacteria and urease. *J. Mater. Civ. Eng.* 26 (12), 04014094. doi:10.1061/(ASCE)MT.1943-5533.0001013
- Zuo, H., Ni, S., and Xu, M. (2023). An assumption of *in situ* resource utilization for “bio-bricks” in space exploration. *Front. Mater.* 10, 1155643. doi:10.3389/fmats.2023.1155643